JACS Au
AN OPEN ACCESS JOURNAL OF THE AMERICAN CHEMICAL SOCIETY

pubs.acs.org/jacsau

Letter

Separation of Cyclohexanone and Cyclohexanol by Adaptive Pillar[5]arene Cocrystals Accompanied by Vapochromic Behavior

Bin Li, Yuan Wang, Lingling Liu, Ming Dong, and Chunju Li*

Cite This: *JACS Au* 2023, 3, 1590−1595

Read Online

ACCESS | Metrics & More | Article Recommendations | Supporting Information

ABSTRACT: The separation of cyclohexanone (CHA-one) and cyclohexanol (CHA-ol) mixtures is of great importance in the chemical industry. Current technology exploits multiple steps of energy-intensive rectification due to their close boiling points. Herein, we report a new and energy-efficient adsorptive separation method employing binary adaptive macrocycle cocrystals (MCCs) built with π-electron-rich pillar[5]arene (P5) and an electron-deficient naphthalenediimide derivative (NDI) that can selectively separate CHA-one from an equimolar CHA-one/CHA-ol mixture with >99% purity. Intriguingly, this adsorptive separation process is accompanied by vapochromic behavior from pink to dark brown. Single-crystal and powder X-ray diffraction analyses reveal that the adsorptive selectivity and vapochromic property are derived from the CHA-one vapor inside the cocrystal lattice voids triggering solid-state structural transformations to yield charge-transfer (CT) cocrystals. Moreover, the reversible transformations make the cocrystalline materials highly recyclable.

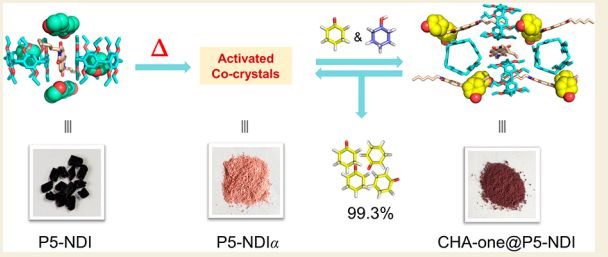

KEYWORDS: *Pillararenes, Exo-wall complexation, Macrocycles, Cocrystals, Adsorption and separation, Vapochromism*

Cyclohexanone (CHA-one) and cyclohexanol (CHA-ol) are important industrial intermediates due to the large demands for them in chemical industry. They are mainly used for manufacturing caprolactam and adipic acid,[1−3] which are key feedstocks for fabricating nylon-6 and nylon-66 polymers in industry. Besides that, CHA-one is also applied as a solvent for resins, paints, and insecticides and CHA-ol serves as a stabilizer and homogenizer for soap emulsions.[4] In industrial production, CHA-one and CHA-ol are produced as a mixture, known as KA-oil, by the air oxidation of cyclohexane or catalytic hydrogenation of phenol.[5−7] The two compounds must be used separately.[8−11] The conventional separation of CHA-one and CHA-ol requires a three-step rectification. This process is very expensive and highly energy-intensive.[12] Therefore, the development of alternative and more energy-conserving ways for separating CHA-one and CHA-ol is significant and necessary.

Recently, macrocycle-based nonporous adaptive crystals (NACs) have emerged as a burgeoning area in supramolecular chemistry, showing great potential in the selective separation of important chemical feedstocks.[13−29] NACs possess the merits of easy preparation, low cost, and good moisture and thermal stability. Very recently, we reported the first example of two-component adaptive macrocycle cocrystals (MCCs) by the marriage of a macrocycle and cocrystal engineering, showing vapochromic behavior to haloalkanes.[30] After that, Huang's group developed another MCC material exhibiting vapochromism after adsorption of alkyl aldehyde vapors.[31] To the best of our knowledge, exploiting MCCs as adsorptive materials for the separation of industrial chemicals has not been reported.

Herein, a new binary MCC was fabricated, exploiting exo-wall binding of perethylated pillar[5]arene (P5) with *N*,*N*′-bis(*n*-hexyl)naphthalenediimide (NDI) driven by charge-transfer (CT) interactions (Scheme 1). The MCC of P5-NDI prepared by cocrystallization in tetrahydrofuran (THF) is black due to the formation of a CT complex between P5 and NDI. P5-NDI cocrystals were activated by heating under reduced pressure to remove THF molecules, resulting in the breakage of CT interactions and the production of a pink cocrystalline material (P5-NDIα) with yellow emission. P5-NDIα is able to selectively separate CHA-one from a CHA-one and CHA-ol mixture (v:v = 50:50) with a purity of 99.3%. Furthermore, the adsorptive separation process was accompanied by vapor-induced vapochromic behavior and crystalline phase structural transformations.

In this system, P5, an important type of building block in solid-state assembly, can be selected as a donor owing to its excellent in-cavity complexation and exo-wall binding capacity.[32−38] NDI was employed as the acceptor because it

Received: March 20, 2023
Revised: April 27, 2023
Accepted: May 1, 2023
Published: May 15, 2023

ACS Publications

© 2023 The Authors. Published by American Chemical Society

https://doi.org/10.1021/jacsau.3c00131
JACS Au 2023, 3, 1590−1595

Scheme 1. Chemical Structures of (a) P5 and NDI and (b) CHA-one and CHA-ol and (c) Electrostatic Potential Maps of P5 and NDI

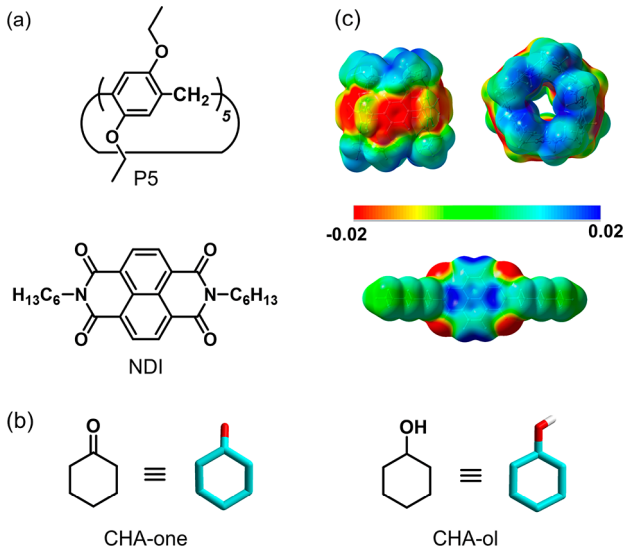

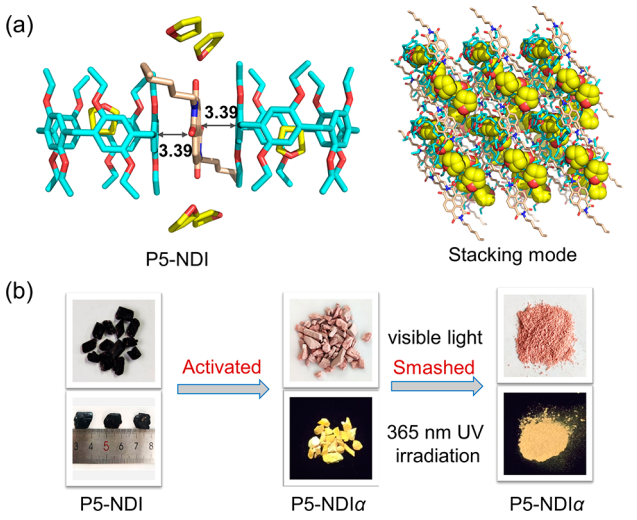

Figure 1. (a) Single-crystal structure of P5-NDI containing THF molecules. Solid lines represent the planar distance of exo-wall $\pi\cdots\pi$ interactions (Å). (b) Schematic representation of P5-NDI and P5-NDIα under visible light and UV light at 365 nm.

is a typical electron-deficient conformer for cocrystals.[39] First, we calculated the electrostatic potential maps of P5 and NDI to analyze the possibility of outside binding. As is shown in Scheme 1c, the highly electronegative aromatic wall of P5 and the strong electropositivity of the aromatic area of NDI proved the complementarity of CT interactions. The MCC of P5-NDI can be prepared on a large scale by slow evaporation of a solution of P5 and NDI (2:1 molar ratio) in THF at room temperature. The black bulk cocrystals with centimeter-scale size were obtained in 1 week (Figure S3). The solid-state ultraviolet−visible (UV−vis) diffuse reflectance spectra and the UV−vis spectra in solution both confirmed the formation of a CT complex, giving rise to an obvious CT absorption band around 520 nm for P5-NDI (Figures S1 and S2). The resulting single-crystal structure showed that P5-NDI adopted the monoclinic space group $P2_1/n$ with two P5, one NDI, and three THF molecules per unit cell (Table S1). NDI molecules are sandwiched between two P5 molecules, forming a 2:1 CT complex by face-to-face $\pi\cdots\pi$ interactions. The interplanar distance was 3.39 Å with a corresponding dihedral angle of 3.07° (Figure 1a). Multiple C−H···O hydrogen bonds between P5 and NDI further stabilize the complex (Figure S4). In molecular packing modes, P5 molecules did not assemble into continuous 1D channels (Figure 1a). THF molecules are not only encapsulated in the P5 cavities by multiple C−H···π interactions but are also stabilized in lattice space between P5 and NDI by forming C−H···O hydrogen bonds with NDI (Figure S5).

Cocrystals of P5-NDI were activated by heating at 75 °C under vacuum and then pulverized to create solvent-free adsorptive materials. Surprisingly, after the removal of solvent molecules, a remarkable color change from black to pink occurred for P5-NDI (Figure 1b). Meanwhile, the resulting material showed yellow luminescence with an emission peak at 578 nm, which was different from those of the crystals of individual P5 and NDI (Figure S6). The solid-state luminescence quantum yield (2.3%) and fluorescence lifetime of activated cocrystals were also determined (Figures S7 and S8). Time-resolved fluorescence measurements revealed that activated cocrystals showed a nanosecond-scale lifetime of 6.59 ns, indicating the solids are fluorescent materials. The radiative decay rate constant (k_r) of activated cocrystals is 3.5×10^6 s^{-1}, far lower than the 1.5×10^8 s^{-1} for the nonradiative decay rate constant (k_{nr}). UV−vis diffuse reflectance spectroscopy displayed no obvious CT band in the activated cocrystals (Figure 2b), indicating the destruction of CT interactions between P5 and NDI by desolvation. ^{1}H NMR suggested a 2:1 stoichiometric ratio of P5 and NDI without solvent (Figure S9). The powder X-ray diffraction (PXRD) pattern revealed that activated P5-NDI still maintained a crystalline state which differed from those of experimental and simulated patterns from the single-crystal structure of the original P5-NDI (Figure S10), suggesting the generation of a new and unknown crystalline phase (P5-NDIα). Thermogravimetric analysis (TGA) indicated no weight loss for P5-NDIα below 300 °C, supporting its high stability (Figure S11). The N_2 sorption isotherm experiment at 77 K confirmed that P5-NDIα was relatively nonporous (S_{BET} = 3.25 m^2 g^{-1}, Figure S12).

Single-component solid−vapor sorption experiments were performed to test the sorption capacity of P5-NDIα toward CHA-one or CHA-ol. As shown in Figures S13 and S14, P5-NDIα took up CHA-one vapor with an adsorption ratio of nearly 2 CHA-one/P5-NDI after saturation, whereas no uptake of CHA-ol was found (Figures S15−S18). Intriguingly, P5-NDIα displayed distinct vapochromism to CHA-one in the adsorption process. Exposing P5-PDIα to CHA-one vapor led to a color change from pink to dark brown as well as fluorescence quenching (Figure 2a). By contrast, after exposure to CHA-ol, no color alteration took place (Figure 2a). UV−vis diffuse reflectance spectroscopy of the colored solids showed a broad absorption band around 524 nm, which can be considered a typical intermolecular CT band (Figure 2b). These results suggested that the capture of CHA-one vapor triggered the formation of the CT complex. The adsorption of CHA-one or CHA-ol molecules was further confirmed by TGA experiments (Figures S19 and S20). TGA curves showed an obvious mass loss of 13.53% for CHA-one (calculated to be 2.0 CHA-one molecules per P5-NDI) and a small weight loss for CHA-ol. For comparison, individual activated P5 or NDI crystals did not absorb CHA-one or CHA-ol (Figures S21−

https://doi.org/10.1021/jacsau.3c00131
JACS Au 2023, 3, 1590−1595

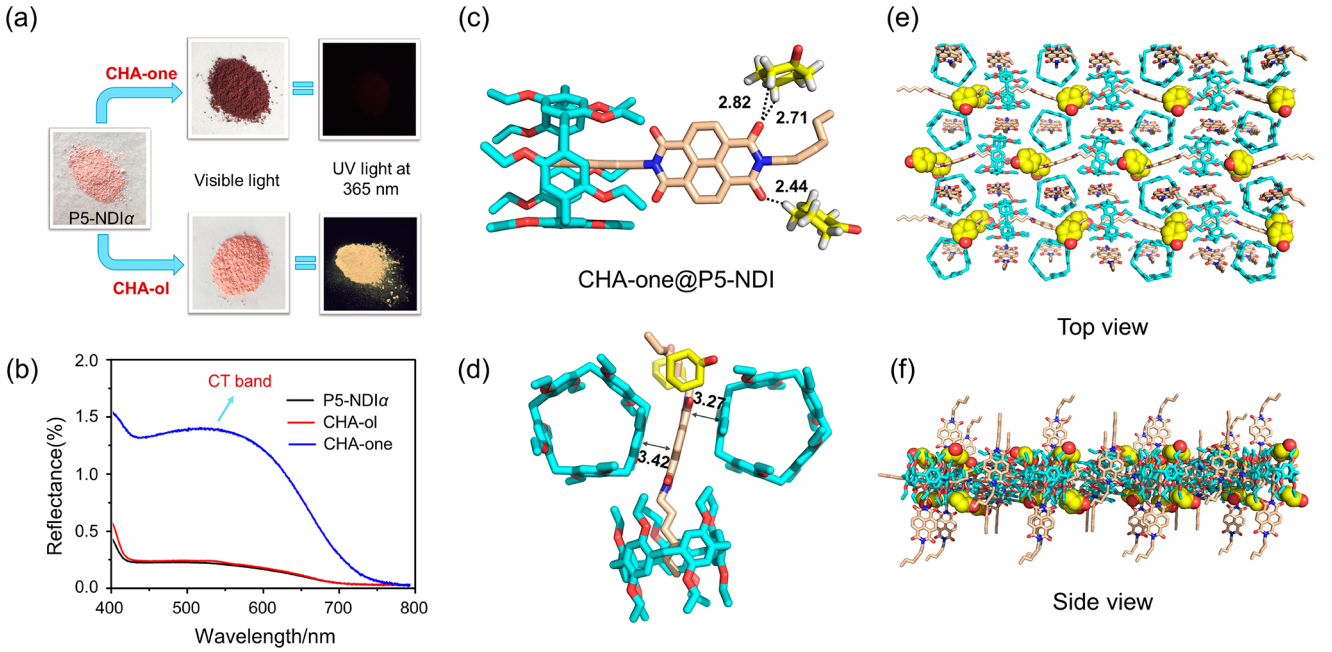

Figure 2. (a) Photographs of P5-NDIα after exposure to CHA-one and CHA-ol vapors under visible light and UV light at 365 nm. (b) Diffuse reflectance spectra of P5-NDIα upon capture of CHA-one and CHA-ol vapors. (c, d) Single-crystal structure of CHA-one@P5-PDI. (e, f) The stacking modes of CHA-one@P5-PDI at different views.

S24). PXRD patterns of P5-NDIα before and after uptake of CHA-one were significantly different, meaning the formation of a new crystalline phase upon the capture of CHA-one (Figure S25). Meanwhile, no diffraction change was found for P5-NDIα after taking in CHA-ol vapor (Figure S26).

To elucidate the mechanism for the adsorption of CHA-one by P5-NDIα with vapor-induced vapochromism and structural transformations, black cocrystals of CHA-one@P5-NDI were crystallized from CHA-one at 50 °C by slow evaporation (Figure S27). An X-ray diffraction analysis revealed that CHA-one@P5-NDI crystallized in the orthorhombic $P2_12_12_1$ space group including two CHA-one molecules in the asymmetric unit (Table S2), which is agreement with the uptake capacity. In the crystal structure, both endocavity inclusion complexation and exo-wall binding interactions between P5 and NDI were observed (Figure 2c,d): i.e., the hexyl chain at one end of the NDI molecule threaded into the P5 cavity to form an inclusion complex by multiple C−H···π and C−H···O interactions (Figure S28), and the skeleton of NDI was sandwiched by two adjacent P5 molecules by face-to-face π···π interactions (Figure 2d and Figure S28). CHA-one molecules were stabilized in the interstices driven by multiple C−H···O interactions with NDI and P5 (Figure 2e,f and Figures S29 and S30). The PXRD pattern of P5-NDIα after uptake of CHA-one is almost the same as the simulated and experimental patterns of CHA-one@P5-NDI (Figure 3c and Figure S31), demonstrating that adsorbing CHA-one brought about the structural transformation in the solid state from P5-NDIα to CHA-one@P5-NDI. Briefly, CHA-one, as a linker of P5 and NDI molecules through noncovalent interactions, facilitates the formation of a CT complex.

Considering the single-component sorption performance, we measured the capability of P5-NDIα to separate a CHA-one/CHA-ol mixture. A time-dependent solid (P5-NDIα)−vapor (an equimolar CHA-one/CHA-ol mixture) sorption experiment was conducted. As expected, P5-NDIα displayed

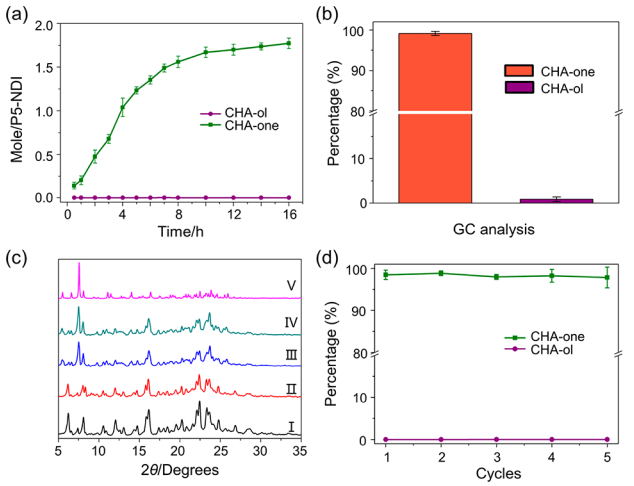

Figure 3. (a) Time-dependent P5-NDIα solid−vapor sorption plots for a 50:50 (v:v) CHA-one/CHA-ol mixture. (b) Relative uptakes of CHA-one and CHA-ol adsorbed by P5-NDIα over 12 h determined by gas chromatography. (c) PXRD patterns of P5-NDIα: (I) original P5-NDIα; (II) after uptake of CHA-ol vapor; (III) after uptake of CHA-one vapor; (IV) after uptake of CHA-one/CHA-ol mixed vapor; (V) simulated from single-crystal structure of CHA-one@P5-NDIα. (d) Relative uptakes of CHA-one and CHA-ol by P5-NDIα after 5 recycles.

exclusive uptake of CHA-one with nearly two CHA-one/P5-NDI after saturation while the uptake quantity of CHA-ol was completely negligible (Figure 3a), consistent with the aforementioned single-component adsorptions. These results demonstrated the high adsorption selectivity of P5-NDIα for CHA-one. Gas chromatography (GC) confirmed that the percentage of CHA-one adsorbed in P5-NDIα was 99.3% (Figure 3b and Figure S32). In addition, P5-NDIα after capture of the mixed vapor also exhibited the same PXRD patterns compared to that of single-component uptake of

https://doi.org/10.1021/jacsau.3c00131
JACS Au 2023, 3, 1590−1595

CHA-one (Figure 3c). It was noted that the structure of CHA-one@P5-NDI could transform back to the original structure of P5-NDIα by removal of CHA-one under vacuum at 85 °C for 12 h, suggesting the recyclability of crystalline P5-NDIα materials (Figures S33 and S34). Then, we measured the recycling capacity of P5-NDIα. After five adsorption−desorption cycles, no performance degradation was observed for CHA-one/CHA-ol mixed vapor (Figure 3d).

In summary, we developed a new and energy-saving adsorptive separation strategy exploiting adaptive MCCs to separate CHA-one and CHA-ol for the first time. The MCC was built by an electron-rich macrocycle of P5 and electron-deficient NDI by exo-wall CT complexation. Activated MCC of P5-NDIα separates CHA-one with high purity (>99%) from a CHA-one and CHA-ol mixture through solid−vapor adsorption, accompanied by vapor-induced vapochromic behavior. Single-crystal X-ray diffraction and PXRD analyses revealed that the mechanism of separation and vapochromic behavior derived from vapor-triggered solid-state structural transformations to form CT cocrystals. Moreover, the reversible structural transformations of the adaptive MCC made P5-NDIα recyclable. Considering the large-scale preparation, perfect recycling, and stimuli responsiveness, the MCC material holds great potential for industrial separation. Fabrication of new MCCs for the separation of hydrocarbons is now in progress in our lab.

Methods

Cocrystal Growth. *P5-NDI.* P5 (2.0 g) was mixed with NDI (0.5 g) in THF (40 mL) and dissolved under ultrasonic conditions. The solution was filtered by a syringe equipped with a 0.22-μm filter. Then slow evaporation of the solvent for about 1 week afforded black bulk cocrystals of P5-PDI.

CHA-one@P5-NDI. P5 (20 mg) was mixed with NDI (8.0 mg) in CHA-one (1 mL) and dissolved under ultrasonic conditions. The solution was filtered by a syringe equipped with a 0.22-μm filter. Then slow evaporation of the solvent at 50 °C for about 5 days afforded black cocrystals of CHA-one@P5-NDI.

Preparation of P5-NDIα Materials. The resulting cocrystals of P5-NDI were activated under vacuum at 75 °C for 12 h to produce pink solvent-free crystalline materials of P5-PDIα.

Vapor Adsorption Experiments. The experiments of single-component CHA-one/CHA-ol or a two-component 50:50 (v:v) CHA-one/CHA-ol mixture adsorption were measured by previously described procedures.[40] An open 3 mL vial containing 5.0 mg of P5-NDIα adsorbent was placed in a closed 20 mL vial including 1 mL of CHA-one or CHA-ol or their mixtures. Uptake in the P5-NDIα materials was measured at each time point, by completely dissolving the P5-NDIα in $CDCl_3$ and determining the ratio of CHA-one or CHA-ol to P5-NDI by ^{1}H NMR spectra. Before measurements, the materials were heated at 30 °C to remove the surface physically adsorbed vapor molecules.

Headspace Gas Chromatography. Head space gas chromatographic (HS-GC) measurements were conducted with an Agilent 7890B instrument equipped with an FID detector and a DB-624 column. Samples were analyzed using headspace injections and were carried out by incubating the sample at 70 °C for 5 min followed by sampling 1 mL of the headspace. The following GC method was used: the oven was programmed from 30 °C and ramped in 10 °C min^{-1} increments to 250 °C with a 15 min hold; the injection temperature was 250 °C; the detector temperature was 250 °C; the helium (carrier gas) flow rate was 3.0 mL min^{-1}.[40]

■ ASSOCIATED CONTENT

Supporting Information

The Supporting Information is available free of charge at https://pubs.acs.org/doi/10.1021/jacsau.3c00131.

Experimental details, including preparation and characteristics of MCCs, X-ray crystallographic data, NMR spectra, and other materials (PDF)

Crystallographic data for CCDC 2239397 (CIF)

Crystallographic data for CCDC 2239398 (CIF)

■ AUTHOR INFORMATION

Corresponding Author

Chunju Li − *Key Laboratory of Inorganic−Organic Hybrid Functional Material Chemistry, Ministry of Education, Tianjin Key Laboratory of Structure and Performance for Functional Molecules, College of Chemistry, Tianjin Normal University, Tianjin 300387, People's Republic of China;* orcid.org/0000-0001-7450-4867; Email: cjli@shu.edu.cn

Authors

Bin Li − *Key Laboratory of Inorganic−Organic Hybrid Functional Material Chemistry, Ministry of Education, Tianjin Key Laboratory of Structure and Performance for Functional Molecules, College of Chemistry, Tianjin Normal University, Tianjin 300387, People's Republic of China*

Yuan Wang − *Key Laboratory of Inorganic−Organic Hybrid Functional Material Chemistry, Ministry of Education, Tianjin Key Laboratory of Structure and Performance for Functional Molecules, College of Chemistry, Tianjin Normal University, Tianjin 300387, People's Republic of China*

Lingling Liu − *Key Laboratory of Inorganic−Organic Hybrid Functional Material Chemistry, Ministry of Education, Tianjin Key Laboratory of Structure and Performance for Functional Molecules, College of Chemistry, Tianjin Normal University, Tianjin 300387, People's Republic of China*

Ming Dong − *Key Laboratory of Inorganic−Organic Hybrid Functional Material Chemistry, Ministry of Education, Tianjin Key Laboratory of Structure and Performance for Functional Molecules, College of Chemistry, Tianjin Normal University, Tianjin 300387, People's Republic of China*

Complete contact information is available at: https://pubs.acs.org/10.1021/jacsau.3c00131

Author Contributions

CRediT: **Bin Li** data curation, investigation, writing-original draft; **Yuan Wang** software; **Chunju Li** project administration.

Notes

The authors declare no competing financial interest.

■ ACKNOWLEDGMENTS

This work was supported by the National Natural Science Foundation of China (22201213 and 21971192), the Natural Science Foundation of Tianjin City (22JCQNJC00730 and 20JCZDJC00200), and the Tianjin Municipal Education Commission (2021KJ188).

REFERENCES

(1) Ritz, J.; Fuchs, H.; Kieczka, H.; Moran, W. C. Caprolacatam. *Ullmann's Encyclopedia of Industrial Chemistry*; Wiley-VCH: 2000.
(2) Bellussi, G.; Perego, C. Industrial Catalytic Aspects of the Synthesis of Monomers for Nylon Production. *CATTECH.* **2000**, *4*, 4−16.
(3) Wittcof, H. A.; Reuben, B. G. *Industrial Organic Chemicals*. Wiley: 1996; pp 253−264.
(4) Fisher, W. B.; VanPeppen, J. F. Cyclohexanol and Cyclohexanone. *Kirk-Othmer Encyclopedia of Chemical Technology*; Wiley: 2000.
(5) Castellan, A.; Bart, J. C. J.; Cavallaro, S. Industrial production and use of adipic acid. *Catal. Today.* **1991**, *9*, 237−254.
(6) Dodgson, I.; Griffen, K.; Barberis, G.; Pignatoro, F.; Tauszik, G. Low cost phenol to cyclohexanone process. *Chem. Ind.* **1989**, 830−833.
(7) Liu, H.; Jiang, T.; Han, B.; Liang, S.; Zhou, Y. Selective Phenol Hydrogenation to Cyclohexanone Over a Dual Supported Pd-Lewis Acid Catalyst. *Science.* **2009**, *326*, 1250.
(8) Goldberg, I.; Stein, Z.; Kai, A.; Toda, F. Separation of Cyclohexanol and Cyclohexanone by Complexation with 1,1-Di(p-hydroxyphenyl)cyclohexane and 1,1,6,6-Tetraphenylhexa-2,4-diyne-1,6-diol, and Crystallographies Structural Studies of the Complexes with the Former Host Compound. *Chem. Lett.* **1987**, *16*, 1617−1620.
(9) Okushita, H.; Yoshikawa, M.; Shimidzu, T. Pervaporation of cyclohexane/cyclohexanone/cyclohexanol mixture through polyoxyethylene grafting nylon 6 membrane. *J. Membr. Sci.* **1995**, *105*, 51−53.
(10) Fan, L.; Xue, M.; Kang, Z.; Wei, G.; Huang, L.; Shang, J.; Zhang, D.; Qiu, S. ZIF-78 membrane derived from amorphous precursors with permselectivity for cyclohexanone/cyclohexanol mixture. *Micropor. Mesopor. Mater.* **2014**, *192*, 29−34.
(11) Branco, L. C.; Crespo, J. G.; Afonso, C. A. M. Studies on the Selective Transport of Organic Compounds by Using Ionic Liquids as Novel Supported Liquid Membranes. *Chem. - Eur. J.* **2002**, *8*, 3865−3871.
(12) Chen, F.; Gu, X.; Liu, X.; Mei, X.; Meng, Q.; Miao, Y.; Shen, T.; Wang, A.; Wang, Y.; Yu, A.; Zhao, F. Recycling cyclohexanone and cyclohexanol comprises e.g. adding alcohol-ketone mixture containing cyclohexanone, cyclohexanol, recovering, carrying out dehydrogenation reaction, heating, and post processing, Sedin Ningbo Engineering Company Limited, CN 106083544-A, 2016.
(13) Jie, K.; Zhou, Y.; Li, E.; Huang, F. Nonporous adaptive crystals of pillararenes. *Acc. Chem. Res.* **2018**, *51*, 2064−2072.
(14) Wu, J.-R.; Yang, Y.-W. Synthetic Macrocycle-Based Nonporous Adaptive Crystals for Molecular Separation. *Angew. Chem., Int. Ed.* **2021**, *60*, 1690−1701.
(15) Jie, K.; Liu, M.; Zhou, Y.; Little, M. A.; Pulido, A.; Chong, S. Y.; Stephenson, A.; Hughes, A. R.; Sakakibara, F.; Ogoshi, T.; Blanc, F.; Day, G. M.; Huang, F.; Cooper, A. I. Near-Ideal Xylene Selectivity in Adaptive Molecular Pillar[*n*]arene Crystals. *J. Am. Chem. Soc.* **2018**, *140*, 6921−6930.
(16) Jie, K.; Zhou, Y.; Li, E.; Zhao, R.; Liu, M.; Huang, F. Linear Positional Isomer Sorting in Nonporous Adaptive Crystals of a Pillar[5]arene. *J. Am. Chem. Soc.* **2018**, *140*, 3190−3193.
(17) Jie, K.; Zhou, Y.; Li, E.; Zhao, R.; Huang, F. Separation of Aromatics/Cyclic Aliphatics by Nonporous Adaptive Pillararene Crystals. *Angew. Chem., Int. Ed.* **2018**, *57*, 12845−12849.
(18) Ogoshi, T.; Saito, K.; Sueto, R.; Kojima, R.; Hamada, Y.; Akine, S.; Moeljadi, A. M. P.; Hirao, H.; Kakuta, T.; Yamagishi, T. Separation of linear and branched alkanes using host-guest complexation of cyclic and branched alkane vapors by crystal state pillar[6]arene. *Angew. Chem., Int. Ed.* **2018**, *57*, 1592−1595.
(19) Wu, J.-R.; Yang, Y.-W. Geminiarene: Molecular Scale Dual Selectivity for Chlorobenzene and Chlorocyclohexane Fractionation. *J. Am. Chem. Soc.* **2019**, *141*, 12280−12287.
(20) Wang, Y.; Xu, K.; Li, B.; Cui, L.; Li, J.; Jia, X.; Zhao, H.; Fang, J.; Li, C. Efficient separation of *cis*- and *trans*-1,2-dichloroethene isomers by adaptive biphen[3]arene crystals. *Angew. Chem., Int. Ed.* **2019**, *58*, 10281−10284.
(21) Yang, W.; Samanta, K.; Wan, X.; Thikekar, T. U.; Chao, Y.; Li, S.; Du, K.; Xu, J.; Gao, Y.; Zuilhof, H.; Sue, A. C.-H. Tiara[5]arenes: synthesis, solid-state conformational studies, host-guest properties and application as nonporous adaptive crystals. *Angew. Chem., Int. Ed.* **2020**, *59*, 3994−3999.
(22) Yao, H.; Wang, Y.-M.; Quan, M.; Farooq, M. U.; Yang, L.-P.; Jiang, W. Adsorptive Separation of Benzene, Cyclohexene, and Cyclohexane by Amorphous Nonporous Amide Naphthotube Solids. *Angew. Chem., Int. Ed.* **2020**, *59*, 19945−19950.
(23) Dey, A.; Chand, S.; Maity, B.; Bhatt, P. M.; Ghosh, M.; Cavallo, L.; Eddaoudi, M.; Khashab, N. M. Adsorptive Molecular Sieving of Styrene over Ethylbenzene by Trianglimine Crystals. *J. Am. Chem. Soc.* **2021**, *143*, 4090−4094.
(24) Luo, D.; He, Y.; Tian, J.; Sessler, J. L.; Chi, X. Reversible Iodine Capture by Nonporous Adaptive Crystals of a Bipyridine Cage. *J. Am. Chem. Soc.* **2022**, *144*, 113−117.
(25) Zhao, Y.; Xiao, H.; Tung, C.-H.; Wu, L.-Z.; Cong, H. Adsorptive separation of cyclohexanol and cyclohexanone by nonporous adaptive crystals of RhombicArene. *Chem. Sci.* **2021**, *12*, 15528−15532.
(26) Zhou, H.-Y.; Chen, C.-F. Adsorptive separation of picoline isomers by adaptive calix[3]acridan crystals. *Chem. Commun.* **2022**, *58*, 4356−4359.
(27) Zhou, Y.; Jie, K.; Zhao, R.; Huang, F. *Cis-Trans* Selectivity of Haloalkene Isomers in Nonporous Adaptive Pillararene Crystals. *J. Am. Chem. Soc.* **2019**, *141*, 11847−11851.
(28) Zhou, Y.; Jie, K.; Zhao, R.; Li, E.; Huang, F. Highly Selective Removal of Trace Isomers by Nonporous Adaptive Pillararene Crystals for Chlorobutane Purification. *J. Am. Chem. Soc.* **2020**, *142*, 6957−6961.
(29) Wu, Y.; Zhou, J.; Li, E.; Wang, M.; Jie, K.; Zhu, H.; Huang, F. Selective Separation of Methylfuran and Dimethylfuran by Nonporous Adaptive Crystals of Pillararenes. *J. Am. Chem. Soc.* **2020**, *142*, 19722−19730.
(30) Li, B.; Cui, L.; Li, C. Macrocycle Co-Crystals Showing Vapochromism to Haloalkanes. *Angew. Chem., Int. Ed.* **2020**, *59*, 22012−22016.
(31) Wang, M.; Li, Q.; Li, E.; Liu, J.; Zhou, J.; Huang, F. Vapochromic Behaviors of A Solid-State Supramolecular Polymer Based on Exo-Wall Complexation of Perethylated Pillar[5]arene with 1,2,4,5-Tetracyanobenzene. *Angew. Chem., Int. Ed.* **2021**, *60*, 8115−8120.
(32) Ogoshi, T.; Yamagishi, T.-a.; Nakamoto, Y. Pillar-Shaped Macrocyclic Hosts Pillar[*n*]arenes: New Key Players for Supramolecular Chemistry. *Chem. Rev.* **2016**, *116*, 7937−8002.
(33) Ohtani, S.; Kato, K.; Fa, S.; Ogoshi, T. Host-Guest Chemistry Based on Solid-State Pillar[*n*]arenes. *Coord. Chem. Rev.* **2022**, *462*, 214503.
(34) Wang, S.; Wang, Y.; Chen, Z.; Lin, Y.; Weng, L.; Han, K.; Li, J.; Jia, X.; Li, C. The marriage of endo-cavity and exo-wall complexation provides a facile strategy for supramolecular polymerization. *Chem. Commun.* **2015**, *51*, 3434−3437.
(35) Lou, X.-Y.; Yang, Y.-W. Pyridine-Conjugated Pillar[5]arene: From Molecular Crystals of Blue Luminescence to Red-Emissive Coordination Nanocrystals. *J. Am. Chem. Soc.* **2021**, *143*, 11976−11981.
(36) Li, M.; Liu, Y.; Shao, L.; Hua, B.; Wang, M.; Liang, H.; Khashab, N. M.; Sessler, J. L.; Huang, F. Pillararene-Based Variable Stoichiometry Co-Crystallization: A Versatile Approach to Diversified Solid-State Superstructures. *J. Am. Chem. Soc.* **2023**, *145*, 667−675.
(37) Mi, Y.; Ma, J.; Liang, W.; Xiao, C.; Wu, W.; Zhou, D.; Yao, J.; Sun, W.; Sun, J.; Gao, G.; Chen, X.; Chruma, J. J.; Yang, C. Guest-Binding-Induced Interhetero Hosts Charge Transfer Crystallization: Selective Coloration of Commonly Used Organic Solvents. *J. Am. Chem. Soc.* **2021**, *143*, 1553−1561.
(38) Li, M.; Hua, B.; Liang, H.; Liu, J.; Shao, L.; Huang, F. Supramolecular Tessellations via Pillar[*n*]arenes-Based Exo-Wall Interactions. *J. Am. Chem. Soc.* **2020**, *142*, 20892−20901.

https://doi.org/10.1021/jacsau.3c00131
JACS Au 2023, 3, 1590−1595

(39) Beldjoudi, Y.; Narayanan, A.; Roy, I.; Pearson, T. J.; Cetin, M. M.; Nguyen, M. T.; Krzyaniak, M. D.; Alsubaie, F. M.; Wasielewski, M. R.; Stupp, S. I.; Stoddart, J. F. Supramolecular Tessellations by a Rigid Naphthalene Diimide Triangle. *J. Am. Chem. Soc.* **2019**, *141*, 17783−17795.
(40) Jie, K.; Liu, M.; Zhou, Y.; Little, M.; Bonakala, S.; Chong, S.; Stephenson, A.; Chen, L.; Huang, F.; Cooper, A. I. Styrene Purification by Guest-Induced Restructuring of Pillar[6]arene. *J. Am. Chem. Soc.* **2017**, *139*, 2908−2911.

https://doi.org/10.1021/jacsau.3c00131
JACS Au 2023, 3, 1590−1595